

Data-Driven Flow and Injection Estimation in PMU-Unobservable Transmission Systems

Satyaprajna Sahoo, *Student Member, IEEE*, Anwarul Islam Sifat, *Member, IEEE*, and Anamitra Pal, *Senior Member, IEEE*

Abstract—Fast and accurate knowledge of power flows and power injections is needed for a variety of applications in the electric grid. Phasor measurement units (PMUs) can be used to directly compute them at high speeds; however, a large number of PMUs will be needed for computing *all* the flows and injections. Similarly, if they are calculated from the outputs of a linear state estimator, then their accuracy will deteriorate due to the quadratic relationship between voltage and power. This paper employs machine learning to perform fast and accurate flow and injection estimation in power systems that are sparsely observed by PMUs. We train a deep neural network (DNN) to learn the mapping function between PMU measurements and power flows/injections. The relation between power flows and injections is incorporated into the DNN by adding a linear constraint to its loss function. The results obtained using the IEEE 118-bus system indicate that the proposed approach performs more accurate flow/injection estimation in *severely* unobservable power systems compared to other data-driven methods.

Index Terms—Flow and Injection estimation, Machine learning (ML), Phasor measurement unit (PMU), Unobservability.

I. INTRODUCTION

Knowledge of active power flows and power injections is fundamental for the reliable, resilient, and economic operation of the electric grid. Traditionally, their knowledge had been used to determine the cost for buying/selling energy as well as for performing vulnerability/security assessment [1], [2]. More recently, with the growing frequency and intensity of extreme weather events as well as increasing penetration of renewable energy resources, a need has been felt for *high-speed tracking* of the power flowing through critical equipment, such as transformers, to determine their health [3].

Power flows and injections can be *directly* computed at high speeds from the outputs of a phasor measurement unit (PMU). However, a large number of PMUs will be needed to estimate *all* of them. They can be calculated *indirectly* from the outputs of a linear state estimator. However, the quadratic relationship between voltage and power deteriorates the quality of flow/injection estimates considerably (see Table I in Section II for a sample illustration). This paper presents a physics-inspired machine learning (ML) formulation to perform data-driven power flow and injection estimation in PMU-unobservable power systems. We focus on the transmission system since most of them already have some PMUs installed. However, the proposed methodology is generic enough that it can be applied to distribution systems as well.

Literature Review: In [4], a minimum variance unbiased estimator was developed to calculate the power flows using

This work was supported in part by the National Science Foundation (NSF) grant under Award ECCS-2132904. The authors are with the School of Electrical, Computer, and Energy Engineering (ECEE) at Arizona State University (ASU).

the state estimation approach. However, the analysis was restricted to DC power flows. A linearly constrained least-squares optimization problem was formulated in [5] to estimate nodal power injections that did not violate power flow constraints. However, no information was provided regarding how the formulation could perform high speed estimation in unobservable power systems. A methodology to learn the topology and estimate the injection statistics in distribution systems with unobservable nodes at PMU timescales was developed in [6]. However, it required the unobservable nodes to be non-adjacent, which may not always be the case.

Main Contributions: This paper proposes the use of ML to simultaneously estimate all power flows and injections in a system that is sparsely observed by PMUs. The ML model is built using deep neural networks (DNNs). The flows and injections in a power system are related by the law of conservation of energy. This knowledge is embedded into the DNNs as a *linear constraint*; the resulting ML model is referred to as a physics-inspired constrained-DNN (PIC-DNN). The offline training is performed using slow timescale historical data obtained from the supervisory control and data acquisition (SCADA) system. The online implementation only uses PMU data, ensuring high speed of estimation. The superior performance of the proposed model over classical as well as other ML models is demonstrated for different numbers of PMUs placed in the IEEE 118-bus system.

II. SOURCES OF ERROR IN POWER CALCULATED FROM STATE ESTIMATES

The most traditional way of determining electrical quantities in a power system is through state estimation. The widely used static state estimator provides an estimate of the voltage phasor (magnitude and angle) of every bus of the system. When a system is completely observed by PMUs, then by only employing PMU data one can perform *linear* state estimation (LSE); LSE is faster and more accurate than SCADA-based state estimation [7]. However, there are two issues with computing power flows/injections from the outputs of LSE: (a) quadratic relationship between voltage and power, and (b) non-Gaussian noise in PMU measurements. These two issues are elaborated below.

Quadratic Relationship: Power flowing through a branch located between bus i and bus j , denoted by p_{ij} , is related to the voltages of the two buses by the equation shown below:

$$p_{ij} = g_{ij}(v_i^2 - v_i v_j \cos \delta_{ij}) - b_{ij}(v_i v_j \sin \delta_{ij}) \quad (1)$$

In (1), v_i and v_j denote the voltage magnitudes of buses i and j , δ_{ij} denotes the voltage angle difference between the two

buses, and g_{ij} and b_{ij} are the real and imaginary components of the admittance matrix, respectively. Similarly, the power injection at bus i , denoted by p_i , can be expressed as,

$$p_i = \sum_{j=1}^{br_i} p_{ij} = \sum_{k=1}^{bu} v_i v_k (g_{ik} \cos \delta_{ik} + b_{ik} \sin \delta_{ik}) \quad (2)$$

where br_i denotes the total number of branches incident on bus i , and bu denotes the total number of buses in the system. It is clear from (1) and (2) that power is proportional to the square of the voltage. Therefore, even a small error in the voltage estimates will get amplified when used for calculating the power flows and power injections.

Non-Gaussian Noise: LSE is most commonly performed using the *least squares* method. However, least squares is the solution to the *maximum likelihood estimation* problem under Gaussian noise environments [8]. Recently, it has been demonstrated that PMU data has non-Gaussian noise [9]. This, in combination with the previously-mentioned source of error, implies that an *indirect* estimation of power flows/injections (by finding the voltages first using state estimation) can result in lower accuracy. This implication is further reinforced through a numerical analysis performed on the IEEE 118-bus system. The results are provided in Table I below.

Table I shows the estimation performance (in terms of root mean square error) when the output of a linear state estimator is used to calculate the power flows and injections in the presence of no noise, 1% total vector error (TVE) Gaussian noise, and 1% TVE non-Gaussian noise. The non-Gaussian noise is described by a two-component Gaussian mixture model (GMM); its parameters are given in the last paragraph of Section IV-A. It is observed from the table that the estimation error increased by at least 60% when the distribution of the noise changed from Gaussian to non-Gaussian. Furthermore, a purely PMU-based LSE requires complete observability of the system by PMUs (for obtaining the results shown in Table I, PMUs were placed at 32 optimal locations that completely observed the system [10]). This requirement of complete observability is another concern of the LSE-based approach.

TABLE I
LSE RESULTS FOR VOLTAGE AND POWER ESTIMATES IN IEEE 118-BUS SYSTEM

	No noise	Gaussian noise (1% TVE)	Non-Gaussian noise (1% TVE)
Voltage magnitude (pu)	4.36 e-13	0.0036	0.0060
Voltage angle (degrees)	1.88 e-11	0.1764	0.2890
Power flow (MW)	1.46 e-10	1.3382	2.2273
Power injection (MW)	2.69 e-10	1.3613	2.2912

Note that a PMU measures voltage and current phasors at the location where it is placed (subject to its measurement channel limitations [11]). This means that the outputs of a PMU can be used to *directly* estimate all the power flows (and subsequently the power injections using (2)). However, this translates to the well-known *minimum vertex cover* problem [12], which requires placing even more PMUs than those

required for complete observability for LSE (which is the solution to the *minimum dominating set* problem). For example, PMUs must be placed at 61 locations in the IEEE 118-bus system to estimate all the power flows using only PMU data. In this paper, we employ ML to directly estimate all the power flows and injections at PMU timescales and with reasonable accuracy while placing significantly fewer PMUs.

III. PHYSICS-INSPIRED ML FOR POWER ESTIMATION IN PMU-UNOBSERVABLE SYSTEMS

Data-driven approaches have been shown to attain considerable success for a variety of power system estimation problems [13]. Some popular data-driven approaches include linear regression (LR), support vector regression (SVR), and DNN-based regression. As the linear relation between the input (PMU measurements) and output (power flows and power injections) for transmission systems that are sparsely observed by PMUs is not guaranteed, LR may not be a good fit for the problem considered in this paper. Similarly, the time complexity of SVR is quadratic w.r.t. the number of training samples [14], which makes it challenging to implement it in a large network with wide variations in features. Therefore, we employ DNNs to perform direct estimation of power flows and injections from PMU measurements.

In Section III-A, we show how DNN-based regression can be used to overcome the unobservability problem associated with purely PMU-based estimation. In Section III-B, we embed the physical law that relates flows and injections into the DNN framework to create the proposed PIC-DNN.

A. DNN Regression to Overcome Unobservability

Recently, we have demonstrated the ability of DNNs to perform high-speed time-synchronized static state estimation in distribution systems that are sparingly observed by micro-PMUs [15], [16]. We did this by using the slow timescale historical smart meter data to create a mapping function between the fast timescale micro-PMU measurements and the states. The mapping function was learned using a DNN because it has excellent approximation capabilities. Here, we leverage this concept to perform power flow and injection estimation from sparsely-placed PMUs in transmission systems.

We start by making two assumptions: (1) we have access to historical SCADA data and system information (e.g., topology) for a sufficient time-period (say, a few months), and (2) PMUs are already placed on select buses of the system (say, highest voltage buses). Using historical SCADA data and system information, we solve the power flow problem to produce voltage and current phasor measurements corresponding to the locations where PMUs are placed. The power flow problem also generates the flow and injection information that matches the PMU measurements. Then, we train a DNN whose inputs are the PMU measurements and outputs are the flows and injections. Finally, during online implementation, streaming data from a select few PMUs is fed into the trained DNN to estimate all the flows and injections at PMU timescales. In this way, a DNN can perform purely PMU-based estimation without needing PMUs to completely observe the system. This DNN model is henceforth referred to as a Direct DNN.

B. Incorporating Physics-based Constraints into DNN

The Direct DNN model developed in Section III-A can estimate the power flows and power injections *independently* from the phasor measurements coming from a select few PMUs. However, as seen in (2), the flows and injections are related by the law of conservation of energy. To account for this physical law, we modify the DNN architecture by appending a linear constraint to its loss function; the resulting model, called PIC-DNN, is described below. In the following, small-case letters indicate vectors, upper-case letters indicate matrices, and the symbol $\hat{\cdot}$ indicates estimates.

For an input, z , and output, y , a regular DNN with weights, W , and biases, b , tries to find a function, F , that minimizes the difference between y and \hat{y} , where $\hat{y} = F(z, W, b)$. The Direct DNN model described in Section III-A performs this minimization using a mean squared error (MSE) loss function, where $z = [V ; I]_{n \times 1}$ and $y = [P_f ; P_{in}]_{m \times 1}$. To incorporate the law of conservation of energy into the Direct DNN model, we start by defining the following loss function:

$$\begin{aligned} \min_{W, b} \quad & (y - \hat{y})^2 \\ \text{s.t.} \quad & \hat{P}_{in} = A \times \hat{P}_f \\ \text{where} \quad & A = \begin{bmatrix} a_{11} & a_{12} & \dots & a_{1m_b} \\ a_{21} & a_{22} & \dots & a_{2m_b} \\ \vdots & \ddots & & \vdots \\ a_{(m-m_b)1} & \dots & & a_{(m-m_b)m_b} \end{bmatrix} \end{aligned} \quad (3)$$

In (3), A is a sparse matrix ($a_{ij} \in \{0, 1\}^{(m-m_b) \times m_b}$) which denotes the power flows that must be added to calculate the power injection of a bus, and m_b and $m - m_b$ denote the number of branch power flows and bus power injections in the system, respectively. Now, power injections can be removed from the output features of the DNN and calculated from the power flow estimates in the following way:

$$\hat{y} = B \times \hat{P}_f, \quad B = [\mathbb{I}_{m_b} ; A] \in \{0, 1\}^{m \times m_b} \quad (4)$$

The conversion matrix, B , is the vertical concatenation of an appropriately sized identity matrix with A , and enables us to get both flow and injection estimates. Thus, by modifying the loss function of the conventional DNN in the manner shown in (3) and (4), we are able to simultaneously minimize the error in the estimates of power flows and power injections while also accounting for the law that relates the two.

There are several ways to implement the above-mentioned constrained formulation inside a DNN model. A simple strategy would be to add a convex optimization layer to the model output. However, the inclusion of such a layer will result in solving two different optimization problems simultaneously during training, which can become computationally burdensome. A more intuitive strategy is to add a static layer after the DNN output layer that calculates the combined \hat{y} from the estimated \hat{P}_f and backpropagates the net error. The updated loss function is given by,

$$\begin{aligned} \min_{W, b} \quad & (B^T B)^{-1} B^T (y - B \times \hat{P}_f)^2 \\ \text{where} \quad & \hat{P}_f = F(z, W, b) \end{aligned} \quad (5)$$

The static weight, $(B^T B)^{-1} B^T$, is the Moore–Penrose inverse of the conversion matrix, B . Using (5), we are not only able to reduce the number of DNN output variables to just the power flows but also implicitly include the linear constraints into the loss function without needing a separate convex optimization layer.

Next, the training dataset, y_{train} , which is only composed of the branch power flows, is split into multiple bins in accordance with the variations that occur in the flows. This improves the accuracy of the DNN because it now has to estimate features that have similar variations. The selection of the optimal number of bins, n_{bin} , involves a trade-off. Increasing the number of bins homogenizes the output data, thereby improving the accuracy of the model. However, unrestricted increment in bin count can increase computational burden while decreasing performance utility.

In summary, the two ways in which we modify the Direct DNN model to create the PIC-DNN model are: (1) modifying the loss function to include a linear constraint, and (2) binning y_{train} in accordance with the observed variations in the power flows in the training database. The overall implementation of PIC-DNN is shown in **Algorithm 1**. The results obtained when the PIC-DNN as well as other ML models are used to estimate power flows and injections in the IEEE 118-bus system is provided in the next section.

Algorithm 1 Implementation of PIC-DNN

Input: Noisy measurements, z

Output: Power flow and injection estimates, \hat{y}

```

1: procedure
2:   Define  $A$ ,  $B$ ,  $n_{bin}$ ,  $epoch$ 
3:   Split  $y_{train}$  into  $n_{bin}$  bins
4:   for  $i=1$  to  $epoch$  do
5:     for  $j=1$  to  $n_{bin}$  do
6:        $\hat{p}_j \leftarrow F_j(z, W_j, b_j)$ 
7:     end for
8:      $\hat{P}_f \leftarrow [\hat{p}_1, \hat{p}_2, \dots, \hat{p}_{n_{bin}}]$ 
9:      $\hat{y} \leftarrow B \times \hat{P}_f$ 
10:     $\delta \leftarrow (B^T B)^{-1} B^T (y - \hat{y})^2$ 
11:    backpropagate  $\delta$ 
12:   end for
13: end procedure

```

IV. RESULTS

The proposed PIC-DNN model for power flow and injection estimation was applied to the IEEE 118-bus system. This system has 99 loads, 54 generators, 11 high voltage (HV) buses, and 186 branches. PMUs were assumed to be placed by default on the 11 HV buses such that all the branches coming out of these buses was directly monitored by them. To obtain branch power flows and bus power injections for this system, we solved an AC optimal power flow (ACOPF) using MATPOWER [17]. The process is similar to the approach in [16], where a distribution kernel was fit over historical slow timescale data, and then multiple samples were drawn from it to generate realistic load variation data. For the given

application, the source of slow timescale data was the SCADA system. However, SCADA data is not available for the IEEE 118-bus system. Therefore, we superimposed the variations of similar loads found in the publicly available 2000-bus Synthetic Texas system [18] onto loads of the IEEE 118-bus system. Doing so ensured that our load variations were realistic. Afterward, the outputs of the ACOPF were used to train the ML models. The training and validation database had a size of $20,000 \times n$ and $2,000 \times n$, respectively, while the test database had a size of $6,000 \times n$, where n is the number of phasor measurements.

The performance of five ML models was investigated in this study. The first two models are LR and SVR, with the latter implemented using a radial basis function kernel. The third model was an Indirect DNN. This model first performs state estimation from sparsely-placed PMUs using the methodology proposed in [16], and then computes the flows and injections from the outputs of the state estimator. The fourth model was the Direct DNN described in Section III-A, while the last model was the PIC-DNN developed in Section III-B. The hyperparameters used for the three DNN models are given in Table II. The loss function for the Direct and Indirect DNN models is the MSE, while for the PIC-DNN model we used (5), with $n_{bin} = 5$. Note that the number of neurons in each hidden layer is kept flexible (using the scaling factor, η) to account for the increase in number of input features due to increase in number of PMUs (see Section IV-B).

TABLE II
HYPERPARAMETERS OF DNNs CREATED IN THIS STUDY

Parameter	Value
Layers	3
Neurons in each hidden layer	Number of input features $\times \eta$
Learning rate	1e-3
Number of epochs	200
Activation function	Rectified Linear Unit
Optimizer	Adam
Batch size	64

The simulations done to compare the performance of the five ML models were conducted on a computer with an Intel Core (TM) i7-11800H CPU @2.3GHz with 16GB of RAM and an RTX 3070Ti GPU. The following two case-studies were designed. The first case-study is a comparative analysis between PIC-DNN and other ML models when PMUs are placed on only the 11 HV buses of the test system. In the second case-study, the performance of all five ML models is investigated as more PMUs are added to the system.

A. Case-Study I: Performance Comparison with PMUs placed only on HV buses

In this case-study, the inputs to the ML models are the voltage and currents obtained from PMUs placed on the 11 HV buses of the IEEE 118-bus system. Therefore, the number of phasor measurements is 41 (= 11 voltage phasors + 30 current phasors), i.e., $n = 82$, since one phasor has two components, while the number of active power flows and injections are 490 (= 372 power flows + 118 power injections), i.e., $m = 490$. To ensure the consistency of estimates obtained from the five

ML models, the analysis was repeated 100 times with different random subsets of the test dataset.

The statistics of the error metric (RMSE) for the five ML models are recorded in Table III. The results show that PIC-DNN does better than the other ML models in both the mean value of RMSE across all the flows and injections as well as the variation of RMSE over the 100 trials. For example, the proposed PIC-DNN outperforms others in terms of the mean by at least 15% and in terms of standard deviation by at least 40%; this denotes a significant improvement in both accuracy and consistency of power flow and injection estimates. The poor performance of the Indirect DNN model can be attributed to the quadratic relationship between voltage and power, as highlighted in Section II. The relatively poor performance of SVR is due to the input dataset being restricted to 5,000 samples. This was done to compensate for its (longer) training time, indicating the handicap of using SVR for large datasets as its scalability is a concern [14].

Lastly, note that the results shown in Table III (as well as the last column of Table I and Fig. 1) were obtained when a two-component GMM noise was added to the voltage and current phasors. The mean, standard deviation, and weights of this noise for magnitudes and angles are $(-0.4\%, 0.6\%)$ and $(-0.2^\circ, 0.3^\circ)$, $(0.25\%, 0.25\%)$ and $(0.12^\circ, 0.12^\circ)$, and $(0.4, 0.6)$, respectively. These values corresponded to a 1% TVE error for voltage and current phasors, as mandated in the IEEE/IEC Standard for PMUs [19].

TABLE III
PERFORMANCE COMPARISON OF ML MODELS FOR POWER ESTIMATION IN TERMS OF THEIR ROOT MEAN SQUARE ERROR (RMSE)

ML Model	Mean of RMSE	Standard deviation of RMSE
LR	5.80	0.020
SVR	7.75	0.120
Indirect DNN	8.37	0.020
Direct DNN	5.91	0.024
PIC-DNN	4.92	0.012

B. Case-Study II: Impact of Increase in Number of PMUs

In this case-study, the number of locations where PMUs must be placed is increased one at a time for each of the five ML models to determine how their performance changes with an increase in the number of PMUs in the IEEE 118-bus system. This is a very practical scenario since, with additional investment in grid modernization, power utilities will add more PMUs not only in the lower voltages of the transmission system but also in the distribution system. Therefore, this case-study indicates the improvements in ML-based power flow and injection estimation with an increase in PMU coverage.

The results obtained as the number of locations where PMUs must be placed increased from 11 to 32 is shown in Fig. 1. To ensure fairness in comparison, the next optimal bus location for placing PMUs is determined independently for each ML model. This means that the horizontal axis of Fig. 1 denotes the total number of buses where PMUs are placed; however, the bus names that go with that number can be different for the five ML models. We stopped at 32 because by placing PMUs on that many buses, we could

directly compare the performance of the different ML models with the conventional LSE results (shown in Table I).

From Fig. 1, it can be realized that the proposed PIC-DNN performs better than the other four ML models for higher degrees of unobservability (fewer PMUs). With an increase in the number of PMUs, the performance of LR becomes comparable with the proposed approach (and even better than PIC-DNN for PMUs placed at 30 or more bus locations). This is expected because linear models can successfully express the relations between the inputs and the outputs as the number of sensors increase. Lastly, the superiority of data-driven approaches is realized from the fact that when the number of bus locations where PMUs are placed is 32, both LR and PIC-DNN outperform LSE results with two-component GMM measurement noise by 35% and 28%, respectively.

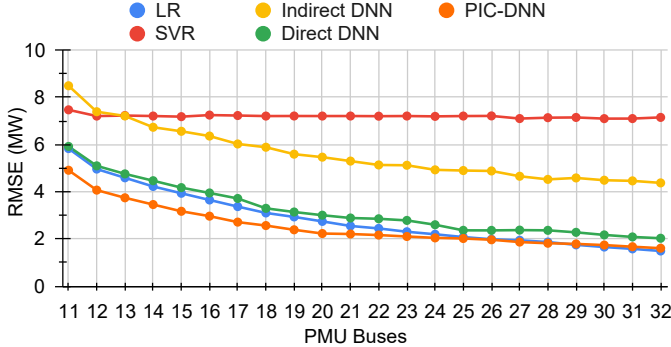


Fig. 1. Performance comparison of ML models with increase in number of PMUs

V. CONCLUSION

This paper proposes a physics-inspired ML approach that uses DNNs to quickly and accurately estimate all the power flows and injections directly from PMUs placed in the transmission system. The proposed PIC-DNN model not only performs consistent estimation when there are very few PMUs in the system but also ensures that the law of conservation of energy is always satisfied. The former is established by intelligently combining inferences drawn from historical SCADA data with real-time PMU data, while the latter is secured by adding a linear constraint to the loss function of the DNN. The results indicate that by placing PMUs on *only 11 buses of the IEEE 118-bus system, PIC-DNN can estimate the flows and injections to within 5 MW of the actual value*, even in the presence of non-Gaussian noise in the PMU measurements. When the PMU locations increase to 32, the estimation error of the proposed approach becomes lower than 2 MW.

The focus of this paper has been on the transmission system. In the future, we plan to extend our analysis to distribution systems where PMUs are gradually being added and for which fast detection of reverse power flows is crucial. We will also combine the outcomes of this research to perform a better security assessment of the power system (e.g., by extending the research of [20]). The DNN models analyzed here had fully-connected feed-forward architectures. We are currently investigating the ability of graph neural networks to better incorporate the physical properties of the power system into ML training and execution (e.g., for ensuring robustness during topology changes).

REFERENCES

- [1] Y. C. Chen and S. V. Dhople, "Tracing power with circuit theory," *IEEE Transactions on Smart Grid*, vol. 11, no. 1, pp. 138–147, 2020.
- [2] R. S. Biswas, A. Pal, T. Werho, and V. Vittal, "A graph theoretic approach to power system vulnerability identification," *IEEE Transactions on Power Systems*, vol. 36, no. 2, pp. 923–935, 2020.
- [3] A. Azmi, J. Jasni, N. Azis, and M. A. Kadir, "Evolution of transformer health index in the form of mathematical equation," *Renewable and Sustainable Energy Reviews*, vol. 76, pp. 687–700, 2017.
- [4] M. Amini, A. I. Sarwat, S. Iyengar, and I. Guvenc, "Determination of the minimum-variance unbiased estimator for DC power-flow estimation," in *IECON 2014-40th Annual Conference of the IEEE Industrial Electronics Society*. IEEE, 2014, pp. 114–118.
- [5] A. Al-Digs, S. V. Dhople, and Y. C. Chen, "Estimating feasible nodal power injections in distribution networks," in *2016 IEEE Power & Energy Society Innovative Smart Grid Technologies Conference (ISGT)*. IEEE, 2016, pp. 1–5.
- [6] D. Deka, M. Chertkov, and S. Backhaus, "Joint estimation of topology and injection statistics in distribution grids with missing nodes," *IEEE Transactions on Control of Network Systems*, vol. 7, no. 3, pp. 1391–1403, 2020.
- [7] P. Chatterjee, A. Pal, J. S. Thorp, and J. De La Ree, "Partitioned linear state estimation," in *2015 IEEE Power & Energy Society Innovative Smart Grid Technologies Conference (ISGT)*, 2015, pp. 1–5.
- [8] A. C. Varghese, A. Pal, and G. Dasarathy, "Transmission line parameter estimation under non-Gaussian measurement noise," *IEEE Transactions on Power Systems*, pp. 1–16, 2022.
- [9] S. Wang, J. Zhao, Z. Huang, and R. Diao, "Assessing Gaussian assumption of PMU measurement error using field data," *IEEE Transactions on Power Delivery*, vol. 33, no. 6, pp. 3233–3236, 2018.
- [10] A. Pal, G. A. Sanchez-Ayala, V. A. Centeno, and J. S. Thorp, "A PMU placement scheme ensuring real-time monitoring of critical buses of the network," *IEEE Transactions on Power Delivery*, vol. 29, no. 2, pp. 510–517, 2013.
- [11] A. Pal, A. K. S. Vullikanti, and S. S. Ravi, "A PMU placement scheme considering realistic costs and modern trends in relaying," *IEEE Transactions on Power Systems*, vol. 32, no. 1, pp. 552–561, 2017.
- [12] J. E. Anderson and A. Chakrabortty, "A minimum cover algorithm for PMU placement in power system networks under line observability constraints," in *2012 IEEE Power and Energy Society General Meeting*, 2012, pp. 1–7.
- [13] M. Khodayar, G. Liu, J. Wang, and M. E. Khodayar, "Deep learning in power systems research: A review," *CSEE Journal of Power and Energy Systems*, vol. 7, no. 2, pp. 209–220, 2021.
- [14] A. Abdiyah and R. Wardoyo, "Time complexity analysis of support vector machines (SVM) in LibSVM," *International Journal Computer and Application*, vol. 128, no. 3, pp. 28–34, 2015.
- [15] B. Azimian, R. S. Biswas, A. Pal, and L. Tong, "Time synchronized state estimation for incompletely observed distribution systems using deep learning considering realistic measurement noise," in *2021 IEEE Power & Energy Society General Meeting*. IEEE, 2021, pp. 1–5.
- [16] B. Azimian, R. S. Biswas, S. Moshtagh, A. Pal, L. Tong, and G. Dasarathy, "State and topology estimation for unobservable distribution systems using deep neural networks," *IEEE Transactions on Instrumentation and Measurement*, vol. 71, pp. 1–14, 2022.
- [17] R. D. Zimmerman, C. E. Murillo-Sánchez, and R. J. Thomas, "MATPOWER: Steady-state operations, planning, and analysis tools for power systems research and education," *IEEE Transactions on Power Systems*, vol. 26, no. 1, pp. 12–19, 2010.
- [18] A. B. Birchfield, T. Xu, K. M. Gegner, K. S. Shetye, and T. J. Overbye, "Grid structural characteristics as validation criteria for synthetic networks," *IEEE Transactions on Power Systems*, vol. 32, no. 4, pp. 3258–3265, 2017.
- [19] IEEE/IEC International Standard - Measuring relays and protection equipment - Part 118-1: Synchrophasor for power systems - Measurements, 2018.
- [20] R. S. Biswas, A. Pal, T. Werho, and V. Vittal, "Mitigation of saturated cut-sets during multiple outages to enhance power system security," *IEEE Transactions on Power Systems*, vol. 36, no. 6, pp. 5734–5745, 2021.